

Time-dependent electron transfer and energy dissipation in condensed media

Elvis F. Arguelles^{1,*} and Osamu Sugino^{1,†}

¹*Institute for Solid State Physics, The University of Tokyo,
5-1-5, Kashiwanoha, Kashiwa, Chiba 277-8581, Japan*

(Dated: March 22, 2024)

Abstract

We study a moving adsorbate interacting with a metal electrode immersed in a solvent using the time-dependent Newns-Anderson-Schmickler model Hamiltonian. We have adopted a semiclassical trajectory treatment of the adsorbate to discuss the electron and energy transfers that occur between the adsorbate and the electrode. Using the Keldysh Green's function scheme, we found a non-adiabatically suppressed electron transfer caused by the motion of the adsorbate and coupling with bath phonons that model the solvent. The energy is thus dissipated into electron-hole pair excitations, which are hindered by interacting with the solvent modes and facilitated by the applied electrode potential. The average energy transfer rate is discussed in terms of the electron friction coefficient and given an analytical expression in the slow-motion limit.

* arguelles@issp.u-tokyo.ac.jp

† sugino@issp.u-tokyo.ac.jp

I. INTRODUCTION

Understanding the fundamental concept of electron transfer has been the subject of intense theoretical research over the past decades due to its importance in a wide-range of fields including physics, chemistry and biology. One of the most widely studied systems is that of atoms or molecules (adsorbates) adsorbed on a metal electrode immersed in a solution. Electron transfer between the adsorbate and the electrode forms the basis of many technologically important electrochemical reactions. It is intrinsically coupled to the vibrational degrees of freedom of the solvent environment, often represented by a phonon bath.

Since the pioneering semiclassical[1, 2] and quantum mechanical[3, 4] studies, the theory of electrochemical electron transfer has progressed over the years. Research on this topic can generally be divided into two categories, depending on the strength of the electronic coupling or the size of the electronic transfer integral. In the strong limit, the characteristic time scales of the adsorbate and the electrode are shorter than those of the solvent, allowing electron transfer to proceed adiabatically[1, 2, 4]. In the weak limit, on the other hand, electron transfer occurs non-adiabatically [3]. Here, "strong" means that the interactions are large enough to establish equilibrium between the adsorbate and the electrode, but are generally weaker relative to the electron-phonon (e-ph) interaction. This is reminiscent of the polaronic system[5, 6] wherein it was argued that the energy shift in proportion to the e-ph couplings must be greater than the electronic couplings to be detected by photoemission experiments.

In recent non-adiabatic formulations[7–11], the restrictions on the strength electronic interactions have been substantially relaxed, allowing for all ranges to be considered. Most theories using time-independent Hamiltonians instead ignore non-adiabatic effects induced by moving adsorbates. In this context, electron transfer rates are calculated at a certain fixed nuclear position of the adsorbate, where electrons have relaxed to their ground state, or in short, within the Born-Oppenheimer picture. This approximation is known to break down even for slow reactant velocities corresponding to the thermal energy, and more so when dealing with metal electrodes where any dynamical processes would lead to electron-hole (e-h) pairs excitations[12].

It is crucial at this stage to distinguish between the concepts of non-adiabaticity in the context of both time-independent and moving adsorbate approaches. In the former

scenario, non-adiabaticity arises from weak electronic interactions in chemical reactions. In models utilizing potential energy surfaces (PES), the electronic interactions are commonly described by the coupling between two diabatic PES[13]. In the latter case, the motion of the adsorbate impedes the relaxation of electrons to the adiabatic ground state, meaning that the electron states become time-dependent and non-adiabatic. Henceforth, we will focus on non-adiabaticity in the context of adsorbate motion.

The charge transfer dynamics on metal substrates is a well studied topic in surface physics mostly on the basis of the time-dependent Newns-Anderson model Hamiltonian[14–19]. Within this model, the time-dependence of adsorbate energy level and the electronic coupling due to the motion of the adsorbate are explicitly considered, yielding many rich and interesting results. For one, the non-adiabatic adsorbate orbital occupancy deviates significantly from the adiabatic value during its encounter with the metal substrate. Further, the energy dissipation through e-h pairs[14, 19–21] and vibrational[22–24] excitations can naturally be included in the model. While the vibrational non-adiabaticity have been previously considered in electrochemical systems [25], the time-dependent electron transfer as well as the effects of continuum of electronic states of the metal electrodes have so far received very little attention.

In the present work, we explore these non-adiabatic effects by employing a time-dependent version of the model Hamiltonian originally introduced by Schmickler[4]. Using the Keldysh formalism, we derive the time-dependent adsorbate orbital occupancy from which the electron and non-adiabatic energy transfer rates can be obtained. The effects of adsorbate velocity and the strength of electron-bath phonon coupling on the electron and energy transfer rates are investigated by numerical calculations. By considering the limit of static adsorbate and high temperature, our formulations are reduced to the Marcus theory (Appendix C). Furthermore, in the limit of slow adsorbate motion, we derive the analytical expressions of the electronic friction coefficient and average energy transfer rate. We discuss the effects of adsorbate electron-solvent modes coupling and electrode potential to the energy exchange and electronic friction. These expressions are then rederived from the e-h excitation probability of the metal electrons, from which, we discuss the adsorbate sticking probability. This work is organized as follows. In II, we present the theoretical model that describes the essential physics of electron transfer in electrochemical systems. This is followed by the derivations of the non-adiabatic orbital occupancy and energy transfer rate in III. We

specialize on the slow motion limit and obtain an analytical expression of the electronic friction coefficient both from the nearly adiabatic expansions of the time-dependent parameters and e-h excitation probability. In IV, we apply the formalism to the electrochemical proton coupled electron transfer reaction where we present some illustrative numerical calculations of the orbital occupancy, and electron and energy transfer rates. Thereupon, we discuss the e-h excitation probability and estimate the sticking probability in the high temperature limit. Finally, we summarize our results and present our conclusions in V.

II. MODEL

The electrochemical system we wish to investigate consists of a moving adsorbate and a metal electrode solvated in a solution. The electron transfer and energy exchange mechanisms of this system are schematically represented in Figure 1. We assume that the system is in equilibrium initially and the adsorbate is located sufficiently far away from the metal electrode so that any electron tunneling is impossible. The ions and atoms comprising the solvent are assumed to move infinitesimally in such a way that they can be represented by harmonic vibrations with infinite modes that form a phonon bath. At distances far from the surface of the electrode, the adsorbate orbital is characterized by a sharp resonance near the Fermi level (ε_F). As the adsorbate approaches the electrode, this state broadens as the energy level crosses ε_F and becomes filled. The broadening is proportional to the square of the electronic overlap integrals between the metal and the adsorbate, represented by the resonance width Δ . In addition, we assume that the adsorbate electron couples with the harmonic solvent modes linearly and shifts the energy level by an amount equivalent to the reorganization energy λ , a quantity proportional to the e-ph interaction. Furthermore, we assume that the adsorbate possesses a kinetic energy initially which is dissipated towards the excitation of e-h pairs in the metal electrode. These excitations consequently induce an electronic frictional force that slows down the adsorbate. There are of course other possible energy dissipation channels. However, in the present work, we are interested in non-adiabatic effects that are unique to a system involving a metal electrode.

In electrochemical systems, the electronic interaction between the metal and adsorbate is generally weak and only one spin state is typically occupied. Therefore, the electron repulsion interaction is neglected in the following. Further, to simplify our calculations, we invoke the

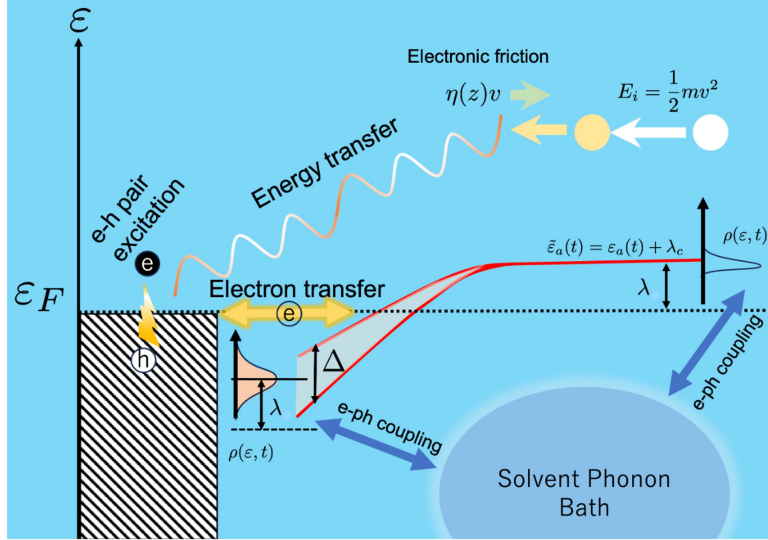


FIG. 1: Schematic diagram of the time-dependent electron transfer and energy exchange in an electrochemical system. An adsorbate with velocity v and initial kinetic energy E_i located far from the metal electrode is characterized by a sharp resonance $\rho(\varepsilon, t)$ and an orbital energy level $\tilde{\varepsilon}_a(t)$ renormalized by the interaction with the solvent modes. The renormalization shifts the orbital energy level above the Fermi level (ε_F) by the reorganization energy λ which quantifies the electron-solvent mode coupling. As the adsorbate moves closer to the surface, $\rho(\varepsilon, t)$ is broadened with a width $\Delta(t)$ due to the electron transfer from the surface. This broadening is accompanied by the occupation of the adsorbate orbital depicted by $\tilde{\varepsilon}_a(t)$ crossing ε_F . In addition, the moving adsorbate induce electron-hole excitations in the metal surface which in turn induce a frictional force $\eta(z)v$ that slows it down.

so-called *trajectory approximation* which assumes that the motion of the adsorbate and the dynamics of the system are separated out. Simply put, the classical trajectory $R(t)$ of the adsorbate is known from the beginning. In most cases, this approximation works well for adsorbates with large masses or moving slowly. Therefore, our work treats the electrons and phonons quantum mechanically, while the adsorbate nuclear dynamics classically. This is justified when the thermal energy is larger than the frequency corresponding to the adsorbate nuclear motion (i.e., $k_B T > \hbar\omega_a$)[26], which we assume to be the case here.

The total Hamiltonian of the system described above may be represented by a time-

dependent version of the Newns-Anderson-Schmickler model[4] ($\hbar = 1$),

$$\begin{aligned}
H(t) = & \varepsilon_a(t)n_a + \sum_k \varepsilon_k c_k^\dagger c_k + \sum_k [V_{ak}(t)a^\dagger c_k + H.c.] \\
& + \sum_q \omega_q b_q^\dagger b_q + (Z - n_a) \sum_q \lambda_q \omega_q (b_q^\dagger + b_q),
\end{aligned} \tag{1}$$

where $n_a = a^\dagger a$. Here, $\varepsilon_a(t) = \varepsilon_a [R(t)]$ is the time-dependent energy level of the adsorbate whose Fock space is spanned by its electron annihilation and creation operators, a and a^\dagger , respectively. ε_k is the band energy of the non-interacting electrons with wavevector k of the metal electrode filled up to the Fermi level, and $c_k(c_k^\dagger)$ are their corresponding annihilation(creation) operators. $V_{ak}(t) = V_{ak} [R(t)]$ is the overlap integral between the metal $|k\rangle$ and moving adsorbate $|a\rangle$ electron states, whose time-dependence is assumed to be separable through $V_{ak}(t) = V_{ak}u(t)$ [18] where, $u(t)$ is some time-dependent function defined in the time domain corresponding to the chosen trajectory $R(t)$. In surface physics literatures, there are several choices for the form of $u(t)$ and here for simplicity we take it as $u(t) = e^{-\gamma|t|^2}$. For a one-dimensional trajectory, $\gamma = \alpha v^2$ where α is the decay constant of the surface wave function and v is the speed of the adsorbate. This choice reflects the fact that empirically, $V_{ak}(t) \propto S$ where S is the overlap between the surface wave function $\psi_k(r)$ and the adsorbate orbital $\phi_a(r - R(t))$. ω_q is the frequency of the harmonic oscillators describing the solvent and $b_q(b_q^\dagger)$ is the annihilation(creation) operator of the phonon of mode q . The harmonic displacements $b_q^\dagger + b_q$ couple linearly to the adsorbate electrons, n_a with coupling strength, λ_q and Z is the charge of the oxidized adsorbate state.

We eliminate the e-ph coupling term in (1) by performing a nonperturbative canonical (Lang-Firsov) transformation $\tilde{H} = e^S H e^{-S}$ where $S = \sum_q \lambda_q n_a (b_q^\dagger - b_q)$. This results in the dressing of the adsorbate electron states as $\tilde{a} = a e^{-\sum_q \lambda_q (b_q^\dagger - b_q)} \equiv aX$, $\tilde{a}^\dagger = a^\dagger e^{\sum_q \lambda_q (b_q^\dagger - b_q)} \equiv a^\dagger X^\dagger$, and the shifting of the phonon operators $\tilde{b}_q = b_q - \lambda_q n_a$, $\tilde{b}_q^\dagger = b_q^\dagger - \lambda_q n_a$ due to the charging effect. The transformation leaves the metal electron states unchanged. The transformed Hamiltonian therefore reads

$$\begin{aligned}
\tilde{H}(t) = & \tilde{\varepsilon}_a(t)n_a + \sum_k \varepsilon_k c_k^\dagger c_k + \sum_k [\tilde{V}_{ak}(t)a^\dagger c_k + H.c.] \\
& + \sum_q \omega_q [b_q^\dagger b_q + Z\lambda_q (b_q^\dagger + b_q)],
\end{aligned} \tag{2}$$

where

$$\tilde{\varepsilon}_a(t) = \varepsilon_a(t) + (2Z - 1)\lambda \quad (3)$$

is the adsorbate orbital energy level renormalized by e-ph coupling through the reorganization energy defined as $\lambda \equiv \sum_q \lambda_q^2 \omega_q$; $\tilde{V}_{ak}(t) = V_{ak}(t)X^\dagger$ is the dressed electronic overlap integral. As in the local polaron problem[27], V_{ak} is usually smaller than λ_q and as a consequence, λ . It is therefore sufficient to replace X^\dagger with its expectation value[28] so that $\tilde{V}_{ak}(t) \approx V_{ak}(t)\langle X^\dagger \rangle = V_{ak}(t) \exp\left[\sum_q \lambda_q^2 (N_q + 1/2)\right]$, where $N_q = \frac{1}{e^{\beta\omega_q} - 1}$ corresponds to the phonon population and $\beta = 1/k_B T$.

III. THEORY

A. Time-dependent electron transfer

To describe the electron transfer, we require the calculation of the time-dependent adsorbate orbital occupancy which can be obtained from Keldysh Green's functions through $\langle n_a(t) \rangle = \text{Im}[G^<(t, t)]$. Our starting point is the nonequilibrium Dyson equation of the Keldysh lesser Green's function

$$G^<(t, t') = G_0^<(t, t') + \int_C dt_1 \int_C dt_2 G_0^<(t, t_1) \Sigma^<(t_1, t_2) G^<(t_2, t') \quad (4)$$

where C is the time contour, $G_0^<$ is the unperturbed lesser Green's function, and $\Sigma^<$ is the self-energy functional. To this end, the contour ordered Green's function of the nonequilibrium system is expressed in a form that allows for a diagrammatic perturbation expansion by virtue of the Wick's theorem. This is achieved by performing a series of transformations to arrive at an expression governed by the solvable, quadratic unperturbed Hamiltonian and a corresponding equilibrium density matrix. By setting the reference time $t_0 \rightarrow -\infty$, and assuming that the initial interactions can be ignored, the contour C can be identified as the Keldysh contour[29] that begins and ends at $-\infty$. The contour integration in (4) is then converted to the real time integration by performing an analytical continuation using Langreth rules[30] resulting in

$$G^< = (1 + G^r \Sigma^r) G_0^< (1 + G^a \Sigma^a) + G^r \Sigma^< G^a, \quad (5)$$

where $G^{r(a)}$ is the retarded(advanced) Green's function, $\Sigma^{r(a)}$ is the retarded(advanced) self-energy, $\Sigma^<$ is the lesser self-energy and $G_0^<$ is the unperturbed lesser Green's function.

The first term is identically zero[31] within the wide-band approximation, which we shall extensively exploit in the following. In integral representation, $G^<$ may be written as[29]

$$G^<(t, t') = \int_{t_0}^t dt_1 \int_{t_0}^{t_1} dt_2 G^r(t, t_1) \Sigma^<(t_1, t_2) G^a(t_2, t'). \quad (6)$$

The lesser self-energy appearing in (6) can be expressed in terms of the the renormalized electronic overlap integrals, $\Sigma^<(t_1, t_2) = \sum_k \tilde{V}_{ak}(t_1) g_k^<(t_1, t_2) \tilde{V}_{ak}^*(t_2)$ with $g_k^<(t_1, t_2) = if(\varepsilon_k) \exp[-i\varepsilon_k(t_1 - t_2)]$ as the unperturbed Green's function of the metal electrode electrons and $f(\varepsilon_k)$ is their corresponding Fermi-Dirac distribution function. In the wide-band limit, the time-independent part of the electronic overlap integrals can be expressed in terms of the adsorbate level resonance width which we assume to be energy-independent through $\Delta = \pi|V_{ak}|^2 \rho(\varepsilon_k)$, with $\rho(\varepsilon_k)$ is the density of states of the metal electrons. Changing the summation over k to an integral over ε , the lesser self-energy takes the form

$$\Sigma^<(t_1, t_2) = i \int d\varepsilon f(\varepsilon) \sqrt{\frac{\Delta(t_1)}{\pi}} \sqrt{\frac{\Delta(t_2)}{\pi}} \exp[-i\varepsilon(t_1 - t_2)] \quad (7)$$

where, $\Delta(t) = \Delta u(t)^2$. Substituting (7) into (6) yields

$$G^<(t, t') = i \int d\varepsilon f(\varepsilon) \int_{t_0}^t dt_1 \sqrt{\frac{\Delta(t_1)}{\pi}} \int_{t_0}^{t_1} dt_2 \sqrt{\frac{\Delta(t_2)}{\pi}} G^r(t, t_1) \exp[-i\varepsilon(t_1 - t_2)] G^a(t_2, t'). \quad (8)$$

As in the polaron systems, we assume that the retarded Green's function can be decoupled as[32]

$$\begin{aligned} G^{r(a)}(t, t') &= \mp i\theta(\pm t \mp t') \langle \{ \tilde{a}(t), \tilde{a}^\dagger(t') \} \rangle_{el} \langle X(t) X^\dagger(t') \rangle_{ph} \\ &= \tilde{G}^{r(a)}(t, t') \langle X(t) X^\dagger(t') \rangle_{ph}. \end{aligned} \quad (9)$$

Here, $X(t) = \exp\left[-\sum_q \lambda_q (b_q^\dagger e^{i\omega t} - b_q e^{-i\omega t})\right]$, and $\langle \dots \rangle_{e(ph)}$ is the expectation value with respect to electrons(phonons). The solvent correlation function $\langle X(t) X^\dagger(t') \rangle_{ph} = \text{Tr} [\rho_{ph} X(t) X^\dagger(t')] \equiv B(t - t')$ is given by

$$B(t) = \exp \left\{ - \sum_q \lambda_q^2 [(N_q + 1)(1 - e^{-i\omega_q t}) + N_q(1 - e^{i\omega_q t})] \right\}. \quad (10)$$

We assume that the solvent bath phonons are characterized by a spectral density $J(\omega) = \sum_{q=1}^N \lambda_q^2 \omega_q^2 \delta(\omega - \omega_q)$. Replacing the q -mode summation with an integration over ω and noting the antisymmetric property of the spectral density, we rewrite (10) as

$$B(t) = \exp \left[\int_{-\infty}^{\infty} d\omega J(\omega) \frac{e^{i\omega t}}{e^{\beta\omega} - 1} \right]. \quad (11)$$

We choose the Drude-Lorentz form of the spectral density

$$J(\omega) = \frac{2\lambda}{\omega_0^2} \frac{\gamma\omega}{\gamma^2 + \omega^2}, \quad (12)$$

where ω_0 is characteristic frequency of the solvent, and γ is the cutoff frequency. λ is typically in the range of 0.5 – 1.0 eV[4]. The ω integration can be performed analytically by contour integration giving

$$B(t) = \exp \left[\sum_{k=0}^{\infty} C_k e^{-\nu_k t} \right], \quad (13)$$

where $C_{k=0} = \frac{\lambda\gamma}{\omega_0^2} [\cot(\frac{\beta\gamma}{2}) - i]$, $C_{k \geq 1} = 4 \frac{\lambda\gamma}{\omega_0^2} \frac{\nu_k}{\beta(\nu_k^2 - \gamma^2)}$, $\nu_0 \equiv \gamma$, and $\nu_k = 2\pi k/\beta$ is the k th Matsubara frequency. In the long time (adiabatic) limit, $B(t) \rightarrow 1$. The Matsubara-decomposed bath correlation function of the form (13) valid for a wide-range of temperature is frequently used in open quantum systems[33–36]. We next write the Dyson equation for \tilde{G}^r as

$$\tilde{G}^r(t, t_1) = G_0^r(t, t_1) + \int d\tau \int d\tau' G_0^r(t, \tau) \Sigma^r(\tau, \tau') \tilde{G}^r(\tau', t_1) \quad (14)$$

where the retarded self-energy is defined as

$$\begin{aligned} \Sigma^r(\tau, \tau') &= \sum_k \tilde{V}_{ak}(\tau) g_k^r(\tau, \tau') \tilde{V}_{ak}^*(\tau') \\ &= -i \int \frac{d\varepsilon}{\pi} \Delta u(\tau) u(\tau') \exp[-i\varepsilon(\tau - \tau')] \theta(\tau - \tau') \\ &= -i \Delta(\tau) \delta(\tau - \tau'). \end{aligned} \quad (15)$$

In the above expression, we used the wide band approximation and the definition of the unperturbed retarded Green's function of the metal electrode $g_k^r(\tau, \tau') = -i\theta(\tau - \tau') \exp[-i\varepsilon_k(\tau - \tau')]$ and \tilde{V}_{ak} . With (15) the integral equation (14) can now be solved[37, 38] yielding

$$\tilde{G}^r(t, t_1) = -i\theta(t - t_1) \exp \left\{ -i \int_{t_1}^t d\tau [\tilde{\varepsilon}_a(\tau) - i\Delta(\tau)] \right\}, \quad (16)$$

where $\tilde{\varepsilon}_a(t)$ is given by (3). The advanced Green's function can also be obtained by following a similar procedure. Inserting (16) and (9) into (8), the time-dependent occupation number $\langle n_a(t) \rangle = \text{Im}[G^<(t, t)]$ may be written as

$$\langle n_a(t) \rangle = \int d\varepsilon f(\varepsilon) |p(\varepsilon, t)|^2, \quad (17)$$

where

$$p(\varepsilon, t) = \int_{t_0}^t dt' \sqrt{\frac{\Delta(t')}{\pi}} B(t') \exp \left\{ -i \int_{t'}^t d\tau [\tilde{\varepsilon}_a(\tau) - i\Delta(\tau) - \varepsilon] \right\}. \quad (18)$$

The above expression can also be derived from the Heisenberg's equations of motion approach as presented in Appendix A. We notice that $|p(\varepsilon, t)|^2$ may be interpreted as the time-dependent projected density of states (PDOS) of the adsorbate in electrochemical systems. The adiabatic expression of the occupation can be derived by ignoring the time dependence of Δ and $\tilde{\varepsilon}_a$. The exponential function may be replaced by $\exp\{-i[\tilde{\varepsilon}_a - i\Delta - \varepsilon](t - t')\}$ and the analytical integration of (18) gives the adiabatic PDOS

$$|p(\varepsilon, t)|^2 \rightarrow \rho^{ad}(\varepsilon) \equiv \frac{1}{\pi} \frac{\Delta}{\Delta^2 + [\tilde{\varepsilon}_a - \varepsilon]^2}, \quad (19)$$

which consequently yields the adiabatic orbital occupancy as

$$\langle n_a^{ad} \rangle = \int d\varepsilon f(\varepsilon) \rho_a^{ad}(\varepsilon). \quad (20)$$

It is more physically meaningful to work in terms of the adsorbate position $R(t)$ rather than time. For simplicity, we neglect any motion parallel to the metal surface and assume that the adsorbate moves at a constant velocity v , such that the one-dimensional trajectory is given by $R(t) \approx z(t) = v|t|$. To describe scattering, one may take $t < 0$ for the incoming (towards the surface) and $t > 0$ as the outgoing portions of the trajectory. The PDOS in (17) is given in the z -representation as

$$\frac{1}{v^2} |p(\varepsilon, z)|^2 = \left| \frac{1}{v} \int_{z_0}^z dz' \sqrt{\frac{\Delta(z')}{\pi}} B(z') \exp \left\{ -\frac{i}{v} \int_{z'}^z dz'' [\tilde{\varepsilon}_a(z'') - i\Delta(z'') - \varepsilon] \right\} \right|^2. \quad (21)$$

Consequently, the adsorbate orbital occupancy can be straightforwardly expressed in the z -representation using (21).

B. Energy dissipation

A moving adsorbate needs to dissipate its kinetic energy to be adsorbed on the surface. Possible dissipation channels under an electrochemical condition are the excitation of vibration in solution and the creation of e-h pairs in metal electrode. With the polaron transformed Hamiltonian (2), let us investigate the total amount of the energy dissipation by integrating the rate of change as derived in Appendix D

$$\dot{\mathcal{E}} = \langle \dot{H} \rangle = \dot{\varepsilon}_a(t) \langle n_a(t) \rangle + \frac{\dot{\Delta}(t)}{\sqrt{\pi\Delta(t)}} \int d\varepsilon f(\varepsilon) \Im[p(\varepsilon, t)], \quad (22)$$

where $p(\varepsilon, t)$ is given by (18). Note that (22) is the same as that derived for vacuum condition[19] with the exception of the renormalized adsorbate energy level and the presence of solvent correlation function in $p(\varepsilon, t)$. On the other hand, the amount of average energy transferred non-adiabatically \bar{E} can be obtained by integrating the rate below, which is derived following the substitution of $\langle n_a(t) \rangle$ with $\langle \delta n_a(t) \rangle = \langle n_a(t) \rangle - \langle n_a^{ad}(t) \rangle$ and $p(\varepsilon, t)$ with $\delta p(\varepsilon, t) = p(\varepsilon, t) - p^{ad}(\varepsilon, t)$

$$\dot{\bar{E}} = \dot{\varepsilon}_a(t) \langle \delta n_a(t) \rangle + \frac{\dot{\Delta}(t)}{\sqrt{\pi\Delta(t)}} \int d\varepsilon f(\varepsilon) \Im[\delta p(\varepsilon, t)]. \quad (23)$$

Just as in the non-adiabatic orbital occupancy, the non-adiabatic average energy transfer rate (23) can be expressed in z -representation by changing the time derivatives to derivatives with respect to z . The resulting expression is valid for all constant values of v . By numerically integrating (21), both $\langle \delta n_a(z) \rangle$ and $\delta p(\varepsilon, z)$ are easily obtained and hence $\dot{\bar{E}}$.

1. Electronic friction coefficient

The e-h excitations near the Fermi level of the electrode induced by the approaching adsorbate give rise to a frictional force that slows it down (see Figure 1). Within the trajectory approximation, the nuclear dynamics is essentially described by the Langevin equation ($m = 1$)

$$\ddot{z}(t) = -\frac{dU(z)}{dz} - \int_{t_0}^t d\tau K(t - \tau)v(\tau) + \zeta(t), \quad (24)$$

where $U(z)$ is the adsorbate-electrode adiabatic potential energy surface, $K(t - \tau)$ is the dissipative nonlocal kernel that depends on the memory of the system and $\zeta(t)$ is the random force. The second term in (24) is the frictional force and is related to $\zeta(t)$ through the fluctuation-dissipation theorem. Since we are interested in the force induced by low energy excitations, we assume that the frictional force is purely electronic. In the limit of slowly moving adsorbate (small $v(t)$), the friction kernel becomes local (Markovian) i.e., $K(t - \tau) = \delta(t - \tau)\eta(t)$, where $\eta(z(t))$ is the electronic friction coefficient. We do not wish to evaluate the full dynamics of adsorbate using (24). Instead, our goal is to derive an expression for the local electronic friction coefficient in the slow motion or equivalently, in the nearly adiabatic limit. Evaluating the frictional force integral in Markovian limit gives

$$\int_{t_0}^t d\tau K(t - \tau)v(\tau) = \eta[z(t)]v(t) \equiv \frac{\dot{\bar{E}}^{SM}}{v(t)}, \quad (25)$$

where,

$$\dot{E}^{SM} = \dot{\tilde{\varepsilon}}_a(t) \langle \delta n_a^{SM}(t) \rangle + \frac{\dot{\Delta}(t)}{\sqrt{\pi\Delta(t)}} \int d\varepsilon f(\varepsilon) \Im[\delta p^{SM}(\varepsilon, t)]. \quad (26)$$

is the average energy transfer rate in the slow motion (SM) limit. For a vanishingly small values of v , t becomes sufficiently large such that $B(t) \sim 1$. Following [19], we proceed by performing Taylor expansions of the time-dependent quantities near their adiabatic values

$$\begin{aligned} \tilde{\varepsilon}_a(t') &\approx \tilde{\varepsilon}_a(t) + (t - t') \dot{\tilde{\varepsilon}}_a(t) \\ \Delta(t') &\approx \Delta(t) + (t - t') \dot{\Delta}(t), \end{aligned} \quad (27)$$

and inserting them into (18) resulting in

$$\begin{aligned} p(\varepsilon, t) &= \sqrt{\frac{\Delta(t)}{\pi}} \int_{-\infty}^0 d\tau \left[1 + i \frac{\dot{E}_a(t)}{2} \tau^2 - \tau \frac{\dot{\Delta}(t)}{2\Delta(t)} \right] \\ &\times \exp \{ -i [E_a(t) - \varepsilon] \tau \}. \end{aligned} \quad (28)$$

where $E_a(t) \equiv \tilde{\varepsilon}_a(t) - i\Delta(t)$. To arrive at (28), we expanded the term proportional to the exponential of the small quantity $\dot{E}_a(t)$ and changed the integration to $\tau = t - t'$ with $t_0 \rightarrow -\infty$. Performing the Gaussian integration of the first term is straightforward and yields the adiabatic expression for p and hence recover $\langle n_{ad} \rangle$ in (20). The succeeding terms in (28) correspond to the non-adiabatic corrections due to the adsorbate motion in SM limit. The nearly adiabatic orbital occupancy then takes the form

$$\begin{aligned} \langle n_a(t) \rangle &= \int d\varepsilon f(\varepsilon) |p^{ad}(\varepsilon, t) + \delta p^{SM}(\varepsilon, t)|^2 \\ &= \langle n_a^{ad}(t) \rangle + \langle \delta n_a^{SM}(t) \rangle, \end{aligned} \quad (29)$$

where $\delta p^{SM}(\varepsilon, t)$ is given by the 2nd and 3rd terms of (28), and the non-adiabatic component of the occupancy $\langle \delta n_a^{SM}(t) \rangle$ in the SM limit may be expressed as

$$\langle \delta n_a^{SM}(t) \rangle = -\pi \int d\varepsilon \frac{df(\varepsilon)}{d\varepsilon} \left\{ \frac{\dot{\Delta}(t)}{\Delta(t)} [\varepsilon - \tilde{\varepsilon}_a(t)] + \dot{\tilde{\varepsilon}}_a(t) \right\} \rho_a^2(\varepsilon, t), \quad (30)$$

from which we obtain the first term of (26). To this end, we discarded the negligible terms proportional to the products $\delta p^{*SM}(\varepsilon, t) \delta p^{SM}(\varepsilon, t)$. We then performed integration by parts, and ignored the negligible first term. Here, $\rho_a(\varepsilon, t)$ is the adsorbate PDOS. Following similar procedure described above, second term of (26) is given by

$$\begin{aligned} \frac{\dot{\Delta}(t)}{\sqrt{\pi\Delta(t)}} \int d\varepsilon f(\varepsilon) \Im[\delta p^{SM}(\varepsilon, t)] &= -\pi \int d\varepsilon \frac{df(\varepsilon)}{d\varepsilon} \frac{\dot{\Delta}(t)}{\Delta(t)} [\varepsilon - \tilde{\varepsilon}_a(t)] \\ &\times \left\{ \frac{\dot{\Delta}(t)}{\Delta(t)} [\varepsilon - \tilde{\varepsilon}_a(t)] + \dot{\tilde{\varepsilon}}_a(t) \right\} \rho_a^2(\varepsilon, t). \end{aligned} \quad (31)$$

Substituting (30) and (31) into (26) yields

$$\dot{E}^{SM} = -\pi \int d\varepsilon \frac{df(\varepsilon)}{d\varepsilon} \left\{ \frac{\dot{\Delta}(t)}{\Delta(t)} [\varepsilon - \tilde{\varepsilon}_a(t)] + \dot{\tilde{\varepsilon}}_a(t) \right\}^2 \rho_a^2(\varepsilon, t). \quad (32)$$

In the z -representation, and by comparing with (25), \dot{E}^{SM} takes the form

$$\dot{E}^{SM}(z(t)) = \eta(z)v^2, \quad (33)$$

where the coefficient of electronic friction is given by

$$\eta(z) = -\pi \int d\varepsilon \frac{df(\varepsilon)}{d\varepsilon} \left\{ \frac{d\Delta(z)}{dz} \frac{[\varepsilon - \tilde{\varepsilon}_a(z)]}{\Delta(z)} + \frac{d\tilde{\varepsilon}_a(z)}{dz} \right\}^2 \rho_a^2(\varepsilon, z). \quad (34)$$

Apart from the presence of the renormalized adsorbate energy level, our above result is equivalent to that of [19]. Further, by setting Δ independent of z , (34) reduces to the expression of the electronic friction coefficient in vacuum[39] where the adsorbate nuclear motion has been considered. In most cases, the relevant electrons that participate in excitation reside near ε_F . We may take the surface temperature to be zero such that the derivative of the Fermi-Dirac distribution becomes a delta function, and the energy integration in (34) is trivial giving

$$\eta(z) = \pi \left\{ \frac{d\Delta(z)}{dz} \frac{[\varepsilon_F - \tilde{\varepsilon}_a(z)]}{\Delta(z)} + \frac{d\tilde{\varepsilon}_a(z)}{dz} \right\}^2 \rho_a^2(\varepsilon_F, z). \quad (35)$$

2. Electron-hole excitation

It is suggestive to investigate how exactly the electron-hole excitations arise from the perspective of the electrons of the metal electrode using the Hamiltonian (1). Working again in the slow-motion limit, the approaching adsorbate is seen by the metal electrons as a slowly varying perturbation[20, 40], which results in instantaneous phase shifts at the Fermi level. This phase shift is related to the electronic friction and hence it is possible to derive (35), provided that the low energy excitations are in the neighborhood of ε_F . Borrowing the methods from surface science, the probability $P(\varepsilon)$ of a system being excited with an energy ε after the perturbation is switched off at $t = \infty$ is[20, 40–42]

$$P(\varepsilon) = \frac{1}{2\pi} \int_{-\infty}^{\infty} dt e^{i\varepsilon t} P(t) \quad (36)$$

where

$$P(t) = \langle \psi(\infty) | \exp \{-i [H(\infty) - E_0] t\} | \psi(0) \rangle. \quad (37)$$

The electrons are assumed to be in their ground state $|\psi(0)\rangle$ at $t = 0$ with an energy $E_0 = \langle \psi(0) | H_0 | \psi(0) \rangle$ before the perturbation was switched on. The excited state $|\psi(\infty)\rangle$ is obtained by applying the time evolution operator $U(\infty, 0)$ to $|\psi(0)\rangle$. Doing so in (37) and switching from Schrödinger to Heisenberg picture, with $H_H(\infty) = U(\infty, 0)H(\infty)U(\infty, 0)$, yields

$$P(t) = \langle \psi(0) | \exp [-iH_H(\infty)t] | \psi(0) \rangle e^{iE_0 t}. \quad (38)$$

To obtain $H_H(\infty)$, we need the expressions for the electron operators c_k^\dagger and c_k in the Heisenberg picture. The procedure is rather lengthy, and we only summarize the important steps and results here. For more details, we refer the readers to the original paper of Brako and Newns in Reference [14]. To proceed, one begins by inserting expression (A11) for annihilation operator a that was derived using equations of motion into (A4) to get c_k . The resulting expressions for c_k is then simplified in the slow limit of the motion. Doing similarly for c_k^\dagger , the electronic Hamiltonian of the metal electrode may be written as

$$H_H(\infty) = \sum_k \varepsilon_k c_k^\dagger(\infty) c_k(\infty) = \frac{i}{2\pi\rho(\varepsilon_k)} \sum_{k', k''} \int dt \int ds \delta(t-s) \dot{F}_{k', k''}(t, s) c_{k''}^\dagger c_{k'}, \quad (39)$$

where $\dot{F}_{k', k''}(t, s) = \frac{\partial}{\partial t} \{ e^{i\varepsilon_{k''} s} e^{-i\varepsilon_{k'} t} e^{-2i[\delta(\varepsilon_{k'}, t) - \delta(\varepsilon_{k''}, s)]} \}$, and $\delta(\varepsilon_k, t) = \arctan \left[\frac{\Delta(t)}{\varepsilon_k - \varepsilon_a(t)} \right]$ is the phase shift. Integrating over s , (39) takes the form

$$H_H(\infty) = H_0 + \sum_{k, k'} U_{k, k'} c_k^\dagger c_{k'}, \quad (40)$$

where $H_0 = \sum_k \varepsilon_k c_k^\dagger c_k$ is the unperturbed Hamiltonian of the metal electrons and $U_{k, k'} = \frac{1}{\pi\rho(\varepsilon_k)} \int dt \dot{\delta}(\varepsilon_k, t) \exp [i(\varepsilon_k - \varepsilon_{k'})t]$ may be considered as an off-shell scattering matrix from state k to k' . The energy difference between the two states $\Omega = \varepsilon_{k'} - \varepsilon_k$ is the e-h excitation energy. Ω is typically small on the order of the inverse of the time scale by which $\dot{\delta}$ varies. Surface electrons that are excited typically reside near the Fermi level so that it is sufficient to replace ε_k by ε_F in $\dot{\delta}$. (40) provides two main ways to calculate $P(t)$: The first is through the linked cluster expansion as done by Brako and Newns in [14], and the second is through Tomononaga bosonization as proposed by Schrönhammer and Gunnarsson [41]. Either method yields the same formally exact expression for $P(t)$ at finite temperature as

$$P(t) = \exp \left\{ \frac{1}{\pi^2} \int_0^\infty d\Omega \Omega |\delta(\Omega)|^2 \left[\coth \left(\frac{\beta\Omega}{2} \right) (\cos \Omega t - 1) - i \sin \Omega t \right] \right\}, \quad (41)$$

where $\delta(\Omega) = \int e^{i\Omega t} \dot{\delta}(\varepsilon_F, t)$. This allows us to calculate $P(\varepsilon)$ through (36). The strength of the delta function of $P(\varepsilon)$ corresponds to the Debye-Waller factor that describes the probability of the system to remain in its ground state. Computing for the second moment of $P(\varepsilon)$ gives the average energy transfer

$$\bar{\varepsilon}(t) = \frac{1}{\pi^2} \int d\Omega \Omega^2 |\delta(\Omega)|^2 = \frac{1}{\pi} \int_{-\infty}^{\infty} dt \dot{\delta}(\varepsilon_F, t)^2. \quad (42)$$

This allows us to write the average energy transfer rate as

$$\dot{\bar{\varepsilon}}(t) = \frac{1}{\pi} \dot{\delta}(\varepsilon_F, t)^2 = \pi \left\{ \frac{\dot{\Delta}(t)}{\Delta(t)} [\varepsilon_F - \tilde{\varepsilon}_a(t)] + \dot{\tilde{\varepsilon}}_a(t) \right\}^2 \rho_a^2(\varepsilon_F, t), \quad (43)$$

which is nothing but energy transfer rate in SM limit (26) at $T = 0$. From (43), the coefficient of electronic friction in (35) is straightforwardly obtained.

IV. APPLICATION

To illustrate the non-adiabatic effects on electron transfer in solvated systems, we apply the above formalism to the case of electrochemical proton ($Z = 1$) discharge on a metal electrode. Such a reaction is described by the well known Volmer process $\text{H}_3\text{O}^+ + e^- \rightarrow \text{H}^* + \text{H}_2\text{O}$ which involves the dissociation of H^+ from H_3O^+ followed by deposition on the metal electrode[3, 43, 44]. This proton coupled electron transfer (PCET) reaction is often treated within the Born-Oppenheimer approximation and assumed to be fully adiabatic, i.e., large electronic overlap between the proton and the electrode. As a consequence, H^+ is almost always guaranteed to be adsorbed. In reality, the motion of the proton affects the electron transfer rate and its fate of being captured by the metal depends upon how it is able to efficiently transfer its kinetic energy towards various energy dissipation channels. We explore the consequences of non-adiabaticity in the following by presenting some illustrative numerical calculations. For simplicity, we omit considerations of bond beaking in H_3O^+ and focus solely on the dynamics of the already dissociated H^+ . The effects of bond breaking were addressed using a position-dependent potential term in a modified version of the Newns-Anderson-Schmickler model[45, 46]. Although one can derive an adiabatic trajectory using this potential term, the essence of non-adiabatic electron transfer dynamics may be captured by starting from a given trajectory whereby the simplest version (1) was derived. In the present case, we ignore the quantum tunneling effects of proton during its transit. Inclusion

of these effects introduces additional complexities that merit a separate discussion, which we plan to address in future works. Additionally, we do not consider adsorption and assume that the proton only scatters upon interacting with the metal. As mentioned earlier, the scattering trajectory is classically described by $R(t) \approx z(t) = v|t|$ where we disregard any motion parallel to the surface. Here, $t < 0$ and $t > 0$ denote incoming (towards the surface) and outgoing (away from the surface) portions of the trajectory, respectively. For convenience, we define the turning point (closest to the electrode) of the trajectory as $z \equiv 0.0$ Bohr. It is important to note that this does not imply direct contact with the surface of the electrode. Considering a proton adsorbate, we assume an initial orbital occupancy $\langle n_a(t_0) \rangle = 0$ and an orbital energy level equal to the Fermi energy (ε_F) which is shifted by λ (*cf.* Figure 1). The time-dependent parameters $\Delta[z(t)]$ and $\tilde{\varepsilon}_a[z(t)]$ are assumed to be Gaussian functions (see Figure 7)

$$\begin{aligned}\Delta(z) &= \Delta \exp(-\alpha z^2) \\ \tilde{\varepsilon}_a(z) &= (\varepsilon_0 - \varepsilon_\infty) \exp(-\kappa z^2) + \varepsilon_\infty + \lambda\end{aligned}\tag{44}$$

where $\alpha = \kappa = 0.015 \alpha_0^{-2}$ (α_0 is the Bohr radius) is a parameter describing the decay of the electrode's wavefunction into the solvent. $\Delta = 0.01$ eV and $\varepsilon_0 = -1.5$ eV are the values of the resonance width and adsorbate energy level at $z = 0.0$ Bohr, and $\varepsilon_\infty = \varepsilon_F = 0.0$ eV is the value of energy level when $z = \infty$. $\Delta(z)$ is maximum at $z = 0.0$ Bohr and 0 at $z = \pm\infty$. The parametrization of $\varepsilon(z)$ describes a scenario in which an initially empty adsorbate orbital level crosses ε_F and becomes occupied through the electron transfer from the metal surface. Further details on the numerical evaluation can be found in AppendixB.

A. Time-dependent proton coupled electron transfer

In Figure 2 the plots illustrate the time-dependent PDOS ((21)) obtained at $T = 300$ K. The left- and right-hand sides of $z = 0.0$ Bohr represent the incoming and outgoing portions of the trajectory, respectively. The upper panel demonstrates the effects of velocity; (a) $v = 0.001 \alpha_0 \text{eV}$, (b) $v = 0.01 \alpha_0 \text{eV}$, and (c) $v = 0.1 \alpha_0 \text{eV}$ when $\lambda = 0.5$ eV. It is notable that the intensities are higher for smaller v in accordance with (21). The intensity corresponds to the matching of the energy ε with $\tilde{\varepsilon}_a(z)$ (see (21) or equivalently (B3)), while the matching condition is relaxed because of $i\Delta$. The matching occurs once in the incoming and once in

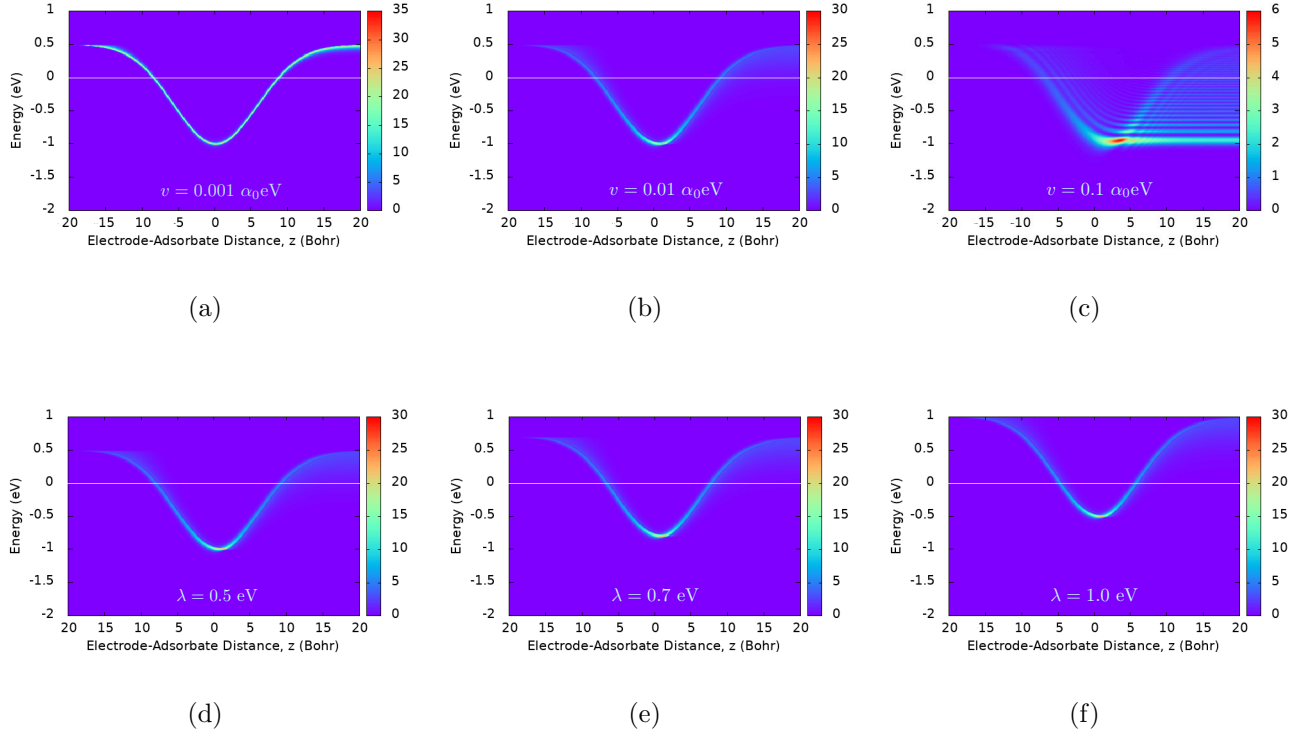
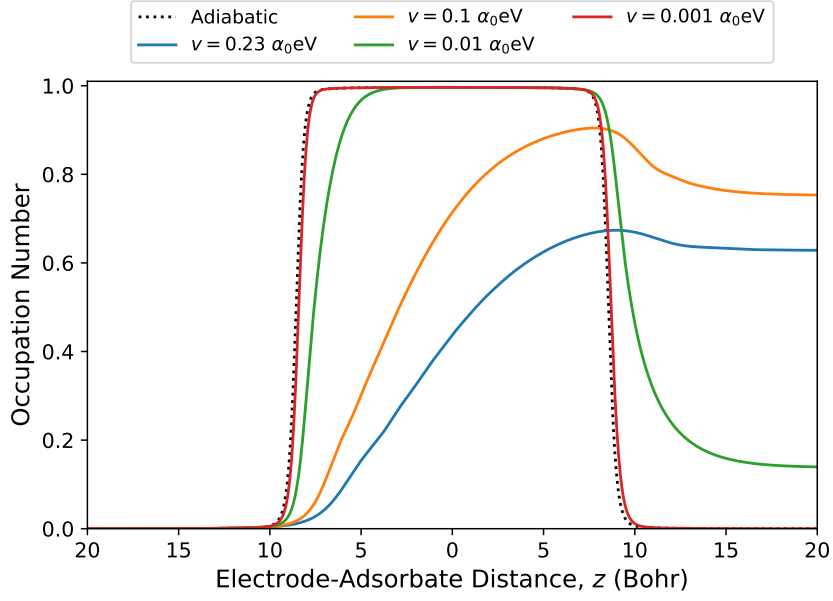
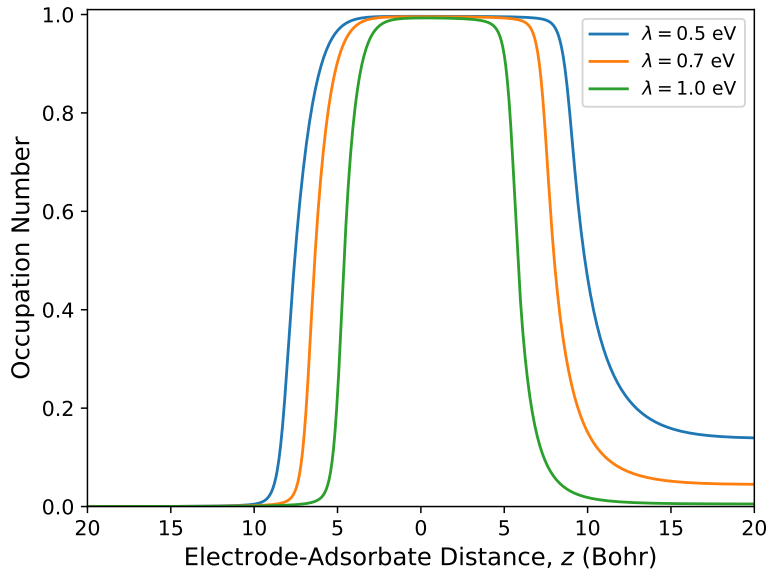


FIG. 2: Time-dependent adsorbate projected density of states (PDOS) for different velocities (a)-(c) at $\lambda = 0.5$ eV and reorganization energies (d)-(e) at $v = 0.01 \alpha_0 \text{eV}$ as functions of energy and adsorbate-electrode distance. The horizontal lines correspond to ε_F . Other parameters are $\Delta = 0.01$ eV, $\varepsilon_0 = -1.5$ eV, $\varepsilon_\infty = \varepsilon_F = 0.0$ eV, $\alpha = \kappa = 0.015 \alpha_0^{-2}$, and $T = 300$ K. The left- and right-hand sides of $z = 0.0$ Bohr correspond to the incoming and outgoing parts of the trajectory, respectively.

the outgoing portions in addition to the case when $z = 0.0$ Bohr. For a slowed adsorbate ($v = 0.001 \alpha_0 \text{eV}$) the PDOS intensities are predominantly localized on a line given by $\varepsilon = \tilde{\varepsilon}_a(z)$. As the adsorbate accelerates (Figure 2c), these intensities become asymmetrically broadened. The asymmetry arises from the retardation of the function $p(\varepsilon, z)$ when v is large. In the lower panel, the effects of the reorganization energy are depicted: (d) $\lambda = 0.5$ eV, (e) $\lambda = 0.7$ eV, and (f) $\lambda = 1.0$ eV when $v = 0.01 \alpha_0 \text{eV}$. The shape of the peak intensities is generally similar to Figure 2b while the intensity is shifted upward by λ as expected from the expression of $\tilde{\varepsilon}_a(z)$, which is the main effect of e-ph coupling. These findings corroborate the behavior of the adsorbate level occupations obtained by integrating the PDOS and the



(a)



(b)

FIG. 3: Adsorbate orbital occupancy at different (a) velocities when $\lambda = 0.5$ eV and (b) reorganization energies when $v = 0.01 \alpha_0 \text{eV}$, using the parameters in Figure 2. The black dotted curves in (a) correspond to the adiabatic orbital occupancy.

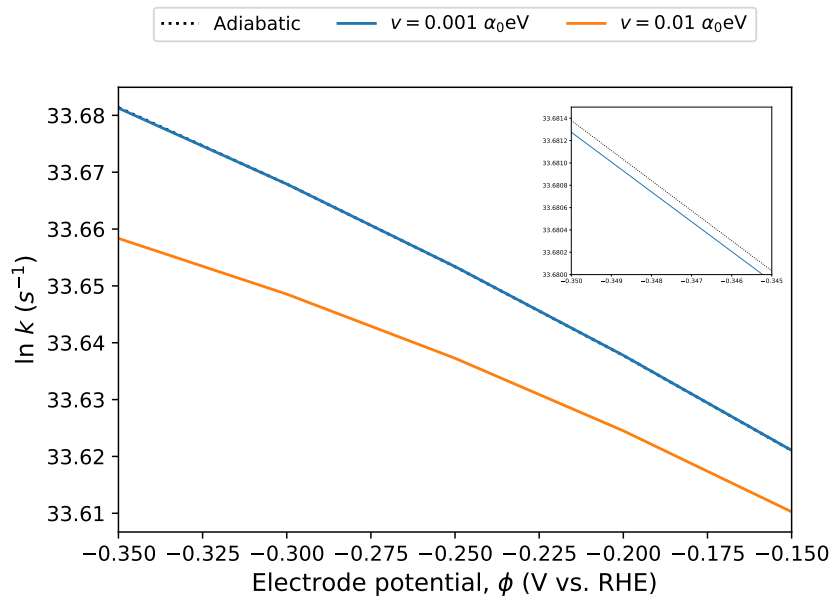
Fermi distribution functions over ε and are shown in Figure 3.

Figure 3a shows the numerically calculated orbital occupancy of proton for different velocities when $\lambda = 0.5$ eV. In the figure, $v = 0.23 \alpha_0\text{eV}$ correspond to the thermal velocity. The adiabatic occupation $\langle n_a^{ad}(z) \rangle$ (dotted lines) is highly symmetric in both incoming and outgoing portions of the trajectory with charge transfer occurring around $z \approx \pm 8.0$ Bohr. Near $z = 0.0$ Bohr, $\langle n_a^{ad}(z) \rangle = 1$ as expected since Δ is small. For non-zero v , the non-adiabatic effects manifest as significant deviations from $\langle n_a^{ad}(z) \rangle$ in both incoming and outgoing portions of the trajectory. This is especially prominent at altitudes where $\tilde{\varepsilon}_a$ crosses ε_F . For faster speeds, the non-adiabatic occupations $\langle n_a(z) \rangle$ are strongly reduced and are extremely asymmetric, with orbital fillings starting to occur closer to $z = 0.0$ Bohr in the incoming trajectory. When $v \geq 0.1 \alpha_0\text{eV}$, the orbital occupancies never reach 1 and are peaked at the outgoing portion. Furthermore, noticeable fractional charge fillings persist long after the proton has left the scattering turning point ($\tilde{\varepsilon}_a(z) \leq \varepsilon_F$). The reduction and asymmetry of $\langle n_a(z) \rangle$ can be easily deduced from the time-dependent PDOS with retardation effects as shown in Figure 2. Physically, these results highlight the inability of the electron system to return to its adiabatic ground state when the adsorbate is in motion; the breakdown of the Born-Oppenheimer approximation. The electronic system relaxation time $\tau \propto 1/\Delta$ becomes large when Δ is small. In electrochemical systems, Δ is typically small, on the order of a few meV implying a much longer τ , and enhanced non-adiabaticity. Performing calculations with increased Δ when $v = 0.1 \alpha_0\text{eV}$ results in the reduction of asymmetric electron transfer. For the case of adsorption in vacuum where Δ usually takes a large value, a slight asymmetry in $\langle n_a(z) \rangle$ is also evident and enhanced by increasing kinetic energy and metal work function[47]. Additional non-adiabatic effects manifest as overfillings of orbital occupancy[18]. For much slower speeds, $\langle n_a(z) \rangle$ approaches the value of $\langle n_a^{ad}(z) \rangle$. When $v = 0.001 \alpha_0\text{eV}$ for example, the non-adiabatic effects are suppressed and the orbital occupancy very nearly coincides with the adiabatic value. This can also be seen in Figure 2a where PDOS retardations are vanishing and the peaks are highly localized. This confirms that our calculations reduce to the adiabatic value in the limit of vanishing velocity.

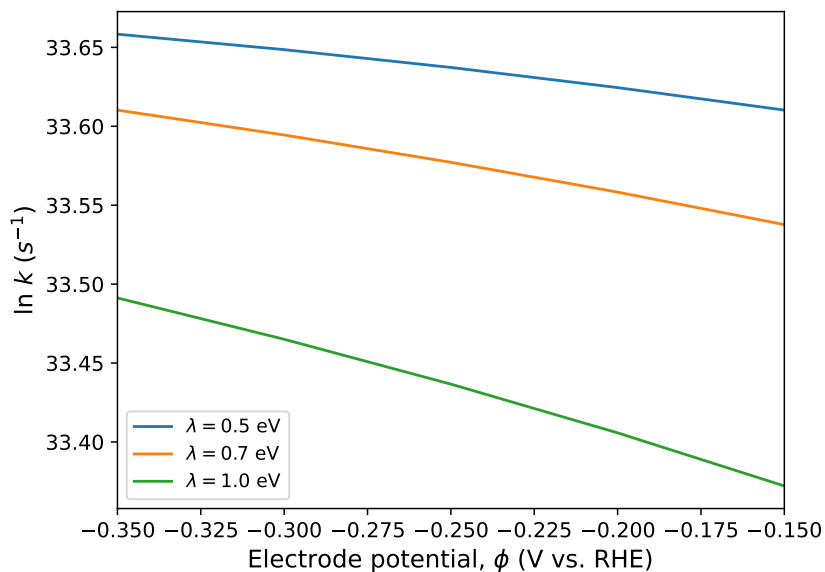
The effects of coupling with the solvent environment are shown in Figure 3b for proton speed of $v = 0.01 \alpha_0\text{eV}$. Within our chosen parameters, $\langle n_a(z) \rangle$ is visibly smaller and narrower when $\lambda = 1.0$ eV, which can be traced back to the behavior of the renormalized energy level depicted in Figure 7b in Appendix B and the time-dependent PDOS with

retardation in Figure 2. At this speed, several delocalized intensities are visible above ε_F (Figure 2b). When λ is increased, these are shifted upwards and do not contribute during ε integration due to the energy range of $f(\varepsilon)$, resulting in narrower orbital occupancy. In contrast, for weaker λ , $\langle n_a(z) \rangle$ are broader due to the Fermi level crossings occurring farther away from $z = 0.0$ Bohr. The persistent partial charge occupations in the outgoing portion are due to the minimal shifting (compared to strong λ) of the PDOS intensities which enables the retardation effects to contribute during ε integrations. When $v = 0.1 \alpha_0 \text{eV}$, the non-adiabatic effects are amplified and the main effects of λ is to reduce the occupation.

We obtain the distance-dependent electron transfer (reduction) rate by dividing the occupation with the electron system's relaxation time $1/2\Delta$, giving $k(z) = 2\Delta(z)\langle n_a(z) \rangle$. The total rate k is the sum of $k(z)$ over the whole path of the adsorbate. Employing similar procedure derives the adiabatic (static) rate k_{ad} from (20). In Appendix C, we show that in the $k_B T \gg \Delta$ limit, k_{ad} reduces to the electron transfer rate in the Marcus theory. Figure 4 shows the electron transfer rates for different v and λ as functions of the electrode potential ϕ vs. reversible hydrogen electrode (RHE). The range of ϕ is chosen to conform with the potential window of experimentally observed reduction rate of proton[48]. The cathodic transfer coefficient α which is proportional to the Tafel slope is observed to decrease (increase) at increasingly (decreasingly) negative ϕ . While we do not aim a quantitative comparison, to within our choice of parameters, we notice that the slopes of our computed k and hence α in both most and least negative regions of ϕ are generally shown to exhibit the same tendencies as the experimental observation. Figure 4a shows that when the velocity is decreased, the electron transfer rate k approaches the adiabatic result for relatively weak coupling with solvent modes ($\lambda = 0.5 \text{ eV}$). Similar conclusions can be drawn for other values of λ . We find that $v = 0.001 \alpha_0 \text{eV}$ is slow enough to closely coincide with k_{ad} . At this speed, the system can be considered as nearly adiabatic. In contrast, higher velocities significantly hinder the electron exchange resulting in the decrease of k . This is especially prominent at thermal velocity $v = 0.23 \alpha_0 \text{eV}$ (not shown) where k is about four times lesser compared to k_{ad} . The effects of coupling with the solvent modes shown in Figure 4b follow closely the results for $\langle n_a(z) \rangle$ at different strengths of λ , i.e., weak (strong) λ results in higher (lower) electron transfer rates. The solvent effectively screens the tunneling electron and renormalizes the adsorbate energy level, resulting in the decrease of orbital occupancy and hence k .



(a)



(b)

FIG. 4: Electron transfer rate for different (a) velocities when $\lambda = 0.5$ eV and (b) reorganization energy when $v = 0.01 \alpha_0 eV$ as a function of electrode potential ϕ in Volts (V) vs. reversible hydrogen electrode (RHE) using the same parameters as in Figure 2. The black dotted line in (a) corresponds to the adiabatic rate and the inset shows the zoomed rate for $-0.350 \leq \phi \leq -0.345$ V vs. RHE

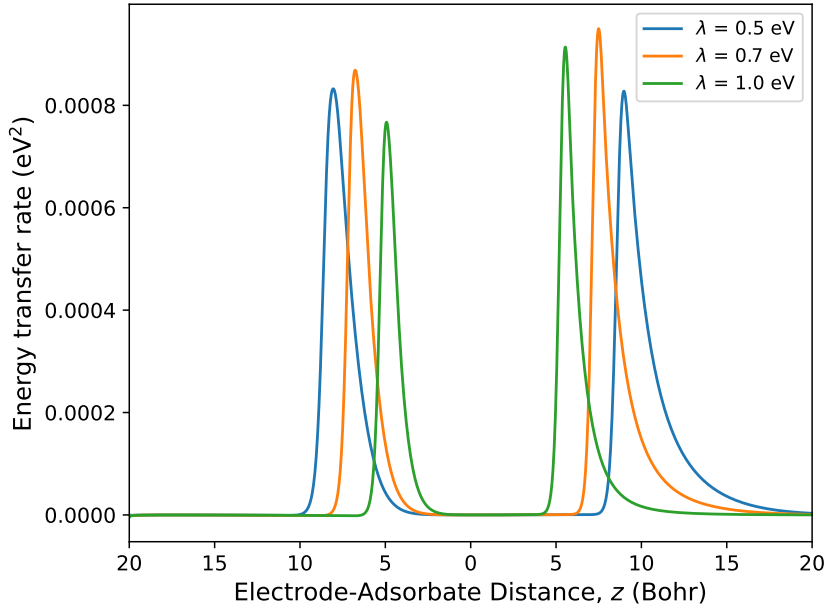


FIG. 5: Average energy transfer rate of an adsorbate scattering on a metal electrode at speed of $v = 0.01 \alpha_0 \text{eV}$ for different strengths of coupling with solvent modes λ . Other parameters are $\Delta = 0.01 \text{ eV}$, $\varepsilon_0 = -1.5 \text{ eV}$, $\varepsilon_\infty = \varepsilon_F = 0.0 \text{ eV}$, and $\alpha = \kappa = 0.015 \alpha_0^{-2}$.

B. Energy transfer

Using the same parameters as in preceding subsection, we numerically evaluate the non-adiabatic average energy transfer rate (23) for $v = 0.01 \alpha_0 \text{eV}$ and different values of λ . The results are shown in Figure 5. For all strengths of λ and in both incoming and outgoing parts of the trajectory, the $\dot{\bar{E}}(z)$ is peaked at the positions where $\tilde{\varepsilon}_a(z) \simeq \varepsilon_F$. The peak position is closer to the turning point ($z = 0.0 \text{ Bohr}$) for stronger λ , in accordance with the position dependent parameters discussed in Appendix B. It was shown[41] previously that the largest contribution to the average energy transfer \bar{E} is proportional to $\sim 1/\Delta$. This implies that \bar{E} is large when the Fermi level crossings occur at distances far from the metal surface, where Δ is small. In our case, \bar{E} can be obtained by integrating (23) over the whole path which yields the following tendency: $\bar{E}(\lambda = 0.5 \text{ eV}) > \bar{E}(\lambda = 0.7 \text{ eV}) > \bar{E}(\lambda = 1.0 \text{ eV})$, i.e., the proton loses more of its kinetic energy when the coupling with the solvent modes is weak. Clearly, from Figure 5, Fermi level crossing occurs farthest from the metal electrode when $\lambda = 0.5 \text{ eV}$, supporting the above average energy loss tendency. Within the trajectory approximation, the effects of velocity to the average energy exchange rate can be indirectly

inferred from Figure 3 and the fact that $\dot{\bar{E}}$ is proportional to $\langle \delta n_a \rangle = \langle n_a \rangle - \langle n_a^{ad} \rangle$. When the adsorbate velocity is small, $\dot{\bar{E}}$ features nearly symmetric peaks centered at distances where Fermi level crossings occur. On the other hand, when the adsorbate moves faster, we notice peculiar energy gains ($\dot{\bar{E}} < 0$) on the way out of the scattering region. This is mainly due to $\langle \delta n_a \rangle$ being negative within this range as can be deduced from the difference $\langle n_a \rangle - \langle n_a^{ad} \rangle$ in Figure 3.

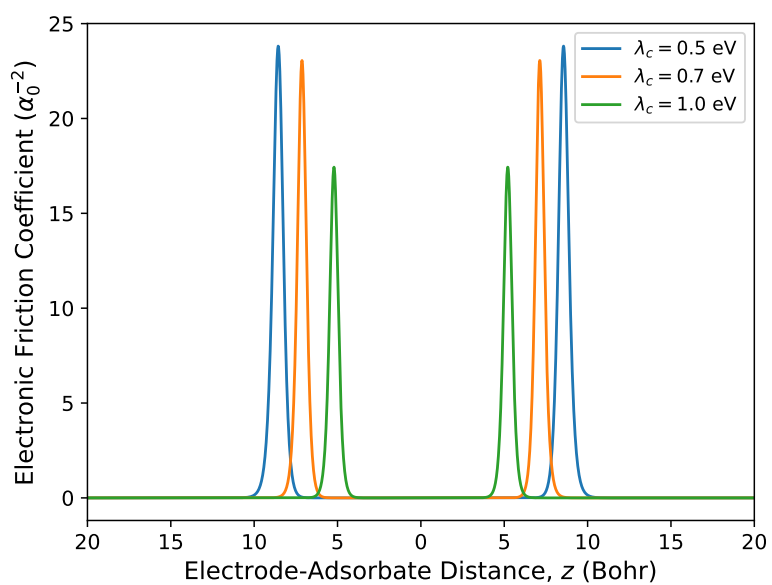
In the slow motion limit, the average energy transfer rate is essentially dictated by the electronic friction coefficient $\eta(z)$ ((34)). Figure 6a shows $\eta(z)$ at $T = 300$ K for different values of the reorganization energy. The curves are highly symmetric in both portions of the trajectory and exhibit similar tendencies with the average energy transfer rate for non-negligible v as seen in Figure 5. The peaks are centered at an adsorbate altitude where the adsorbate energy level crosses the Fermi level. For weak λ , this level crossing occurs at a distance far away from the metal implying significant energy loss toward e-h excitations. The opposite tendency can be deduced when λ is strong in which the peaks are shifted closer to the metal. This can be summarized by integrating $\dot{\bar{E}}^{SM}$ over the whole trajectory to yield the average energy transfer (loss) in the SM limit which results in $\bar{E}^{SM}(\lambda = 0.5 \text{ eV}) > \bar{E}^{SM}(\lambda = 0.7 \text{ eV}) > \bar{E}^{SM}(\lambda = 1.0 \text{ eV})$.

The effects of the electrode potential on the electronic friction coefficient when $\lambda = 0.5$ eV is depicted in Figure 6b. Negative values of the electrode potential ϕ means shifting $\tilde{\varepsilon}_a(z)$ downward relative to ε_F , and then shifting the Fermi level crossings away from the metal electrode. When $\phi = -0.35$ V vs. RHE, for example, $\eta(z)$ is significantly broadened and lowered. This indicates that an increasing ϕ would make the frictional force act on a much wider range of z , thus increasing the average energy transfer. This leads to the important consequence that increasing ϕ promotes the energy loss of an adsorbate and increase the likelihood of trapping on the metal surface.

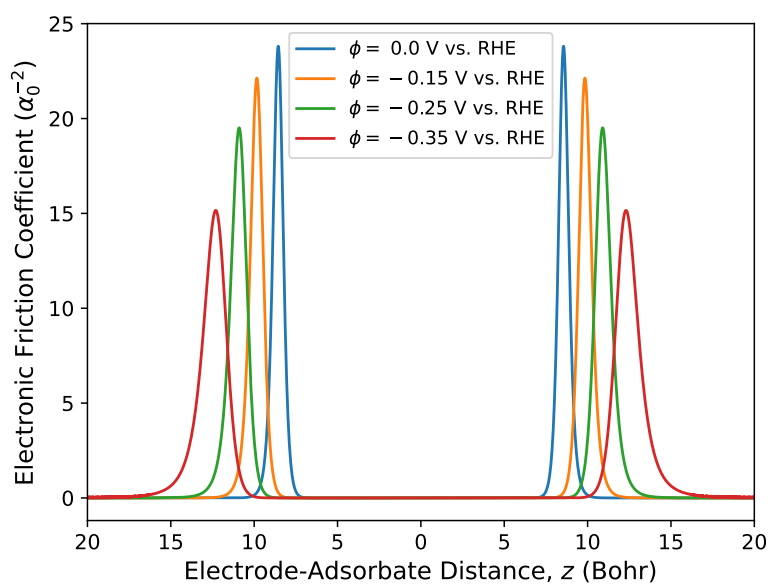
We further remark on the possibility of the proton being captured by the metal surface during their encounter. Assuming that the relevant energy dissipation channel is the e-h excitations in the metal, the sticking probability of the proton can be calculated as

$$S(E_i) = \int_{E_i}^{\infty} P(\varepsilon) d\varepsilon, \quad (45)$$

where E_i is the initial kinetic energy of the proton, and $P(\varepsilon)$ is the e-h excitation probability (36). Roughly speaking, when the average energy loss is larger than E_i , $S \rightarrow 1$, or the proton



(a)



(b)

FIG. 6: Electronic friction coefficient for different (a) λ when electrode potential $\phi = 0.0$ V and (b) ϕ when $\lambda = 0.5$ eV as a function of z . Other parameters are the same as in Figure 5.

is likely to be adsorbed. Without resorting to the full numerical evaluation, it is possible to obtain an analytical form of $P(\varepsilon)$ at least in the high temperature limit. To the leading order, we may introduce approximations as $\coth(\beta\Omega/2) \approx 2/\beta\Omega$, $\cos\Omega t - 1 \approx \Omega^2 t^2/2$ and $\sin\Omega t \approx \Omega t$ when Ω is substantially small. Using these, (41) can be expressed as

$$P(t) \approx \exp(-\bar{\epsilon}k_B T t - i\bar{\epsilon}t), \quad (46)$$

which after evaluating the time integrals in (36) yields a Gaussian form of $P(\varepsilon)$ as

$$P(\varepsilon) = \frac{1}{\sqrt{2\pi\bar{\epsilon}k_B T}} \exp\left[-\frac{(\varepsilon - \bar{\epsilon})^2}{4\bar{\epsilon}k_B T}\right], \quad (47)$$

which is peaked at the values of the average energy transfer rate $\bar{\epsilon}$. If we take $\bar{\epsilon} = \bar{E}^{SM}$ since they are formally equivalent via (35), our estimated tendency for \bar{E}^{SM} suggests that the $P(\varepsilon)$ spectra will be most shifted towards the energy loss portion ($\varepsilon > 0$) for small λ and more negative ϕ . Evaluating (45), using (47) and (43) for $v = 0.001\alpha_0\text{eV}$ gives $S(\lambda = 0.5 \text{ eV}) > S(\lambda = 0.7 \text{ eV}) > S(\lambda = 1.0 \text{ eV})$. This implies that strong λ results in small energy loss and the adsorbate is less likely to be trapped. Conversely, weak λ promotes energy loss and the probability of the adsorbate to stick on the metal surface. We may also infer the effects of electrode potential on the e-h excitation probability and the adsorbate sticking probability. For some values of λ , an increasingly negative ϕ would shift the peaks of $P(\varepsilon)$ towards the loss portion of the spectra. This indicates that the sticking probability of the adsorbate is promoted when ϕ is increased.

V. SUMMARY AND CONCLUSIONS

We have studied the non-adiabatic effects due to the dynamic adsorbate interacting with the metal electrode in the presence of solvent using the time-dependent Newns-Anderson-Schmickler model Hamiltonian. The electron transfer rate is studied in terms of the time-dependent adsorbate occupation derived using the nonequilibrium Green's function formalism and the trajectory approximation. Our numerical calculations show that the electron transfer rate is significantly reduced for nonzero adsorbate velocities and large electron-bath phonons couplings. It is also shown that the rate is strikingly peaked at distances where the adsorbate energy crosses the Fermi level of metal electrode. These crossings occur away from (close to) the metal surface for the small (large) solvent reorganization energy λ . This

results in significant energy loss for weak λ . For small adsorbate velocities, we derived the analytic expression of the electronic friction coefficient $\eta(z)$. $\eta(z)$ is strongly peaked at a distance where Fermi level crossings occur. When the electrode potential is made more negative, the crossing occurs away from the metal surface leading to higher energy transfer rate and hence larger energy loss. We also discussed the probability $P(\varepsilon)$ of the electron system being excited, from which we derived the average energy transfer rate and the coefficient of electronic friction. In the high temperature limit, we discussed the sticking probability obtained from $P(\varepsilon)$. Since $P(\varepsilon)$ is peaked at the average energy loss value, we conclude that the sticking probability is high when λ is small and the electrode potential is high.

VI. ACKNOWLEDGMENTS

This research is supported by the New Energy and Industrial Technology Development Organization (NEDO) project, MEXT as “Program for Promoting Researches on the Supercomputer Fugaku” (Fugaku battery & Fuel Cell Project) (Grant No. JPMXP1020200301, Project No.: hp220177, hp210173, hp200131), Digital Transformation Initiative for Green Energy Materials (DX-GEM) and JSPS Grants-in-Aid for Scientific Research (Young Scientists) No. 19K15397. Some calculations were done using the supercomputing facilities of the Institute for Solid State Physics, The University of Tokyo.

Appendix A: Occupation Number from Equations of Motion Approach

We can recover the results of nonequilibrium Green’s function formalism using equations of motion approach (EOM). The Heisenberg EOM for an operator \hat{O} is given by

$$\frac{d\hat{O}}{dt} = i[\tilde{H}, \hat{O}] \quad (\text{A1})$$

where \tilde{H} is the canonically transformed Hamiltonian. For brevity, we drop the hats on the operators. The EOM of the adsorbate electron annihilation operator is

$$i\frac{d\tilde{a}(t)}{dt} = \tilde{\varepsilon}_a(t)\tilde{a}(t) + \sum_k V_{ak}(t)c_k(t), \quad (\text{A2})$$

with $\tilde{V}_{ak}(t)a^\dagger(t) = V_{ak}(t)\tilde{a}^\dagger(t)$. We also require the EOM of metal electron’s annihilation operator,

$$i\frac{dc_k(t)}{dt} = \varepsilon_k c_k(t) + V_{ak}^*(t)\tilde{a}(t) \quad (\text{A3})$$

Integrating (A3) to solve for c_k gives

$$c_k(t) = \exp[-i\varepsilon_k(t-t_0)] c_k(t_0) - i \int_{t_0}^t dt' \exp[-i\varepsilon_k(t-t')] V_{ak}^*(t') \tilde{a}(t'), \quad (\text{A4})$$

where t_0 is an initial reference time. We substitute this into (A2) to arrive at

$$\begin{aligned} i \frac{d\tilde{a}(t)}{dt} &= \tilde{\varepsilon}_a(t) \tilde{a}(t) + \sum_k V_{ak}(t) \exp[-i\varepsilon_k(t-t_0)] c_k(t_0) \\ &\quad - i \sum_k \int_{t_0}^t dt' \exp[-i\varepsilon_k(t-t')] V_{ak}(t) V_{ak}^*(t') \tilde{a}(t'). \end{aligned} \quad (\text{A5})$$

The last term in (A5) can be evaluated with the aid of the wide band limit resulting to

$$-i \sum_k \int_{t_0}^t dt' \exp[-i\varepsilon_k(t-t')] V_{ak}(t) V_{ak}^*(t') \tilde{a}(t') = -i\Delta(t) \tilde{a}(t), \quad (\text{A6})$$

which then yields

$$i \frac{d\tilde{a}(t)}{dt} = [\tilde{\varepsilon}_a(t) - i\Delta(t)] \tilde{a}(t) + \sum_k V_{ak}(t) \exp[-i\varepsilon_k(t-t_0)] c_k(t_0) \quad (\text{A7})$$

This can be integrated to give

$$\begin{aligned} \tilde{a}(t) &= \exp \left\{ -i \int_{t_0}^t dt' [\tilde{\varepsilon}_a(t') - i\Delta(t')] \right\} \tilde{a}(t_0) + \int_{t_0}^t dt' \exp \left\{ -i \int_{t'}^t d\tau [\tilde{\varepsilon}_a(\tau) - i\Delta(\tau)] \right\} \\ &\quad \times \sum_k V_{ak}(t') \exp[-i\varepsilon_k(t'-t_0)] c_k(t_0). \end{aligned} \quad (\text{A8})$$

Inserting $1 = e^{-\lambda_a(b_q^\dagger - b_q)} e^{\lambda_a(b_q^\dagger - b_q)} \equiv X(t) X^\dagger(t)$ into the second term of (A8) yields

$$\begin{aligned} \tilde{a}(t) &= \exp \left\{ -i \int_{t_0}^t dt' [\tilde{\varepsilon}_a(t') - i\Delta(t')] \right\} \tilde{a}(t_0) + \int_{t_0}^t dt' \exp \left\{ -i \int_{t'}^t d\tau [\tilde{\varepsilon}_a(\tau) - i\Delta(\tau)] \right\} \\ &\quad \times \sum_k \tilde{V}_{ak}(t') X(t') \exp[-i\varepsilon_k(t'-t_0)] c_k(t_0). \end{aligned} \quad (\text{A9})$$

As in the Keldysh formalism, we take $\tilde{V}_{ak}(t') \approx V_{ak}(t') \langle X^\dagger(t') \rangle \equiv \bar{V}_{ak}(t')$ for $V_{ak} \ll \lambda$. At this point, we emphasize the difference between \tilde{V} and \bar{V} . With this, $\tilde{a}(t)$ takes the form

$$\begin{aligned} \tilde{a}(t) &= \exp \left\{ -i \int_{t_0}^t dt' [\tilde{\varepsilon}_a(t') - i\Delta(t')] \right\} \tilde{a}(t_0) + \int_{t_0}^t dt' \exp \left\{ -i \int_{t'}^t d\tau [\tilde{\varepsilon}_a(\tau) - i\Delta(\tau)] \right\} \\ &\quad \times \sum_k \bar{V}_{ak}(t') X(t') \exp[-i\varepsilon_k(t'-t_0)] c_k(t_0). \end{aligned} \quad (\text{A10})$$

Multiplying both sides of (A10) with $X^\dagger(t)$ and using the decoupling approximation in (9), the expectation values with respect to the bath phonons gives

$$\begin{aligned}
a(t) &= \exp \left\{ -i \int_{t_0}^t dt' [\tilde{\varepsilon}_a(t') - i\Delta(t')] \right\} a(t_0) \langle X(t_0)X^\dagger(t) \rangle \\
&+ \int_{t_0}^t dt' \exp \left\{ -i \int_{t'}^t d\tau [\tilde{\varepsilon}_a(\tau) - i\Delta(\tau)] \right\} \\
&\times \sum_k \bar{V}_{ak}(t') B(t' - t) \exp[-i\varepsilon_k(t' - t_0)] c_k(t_0).
\end{aligned} \tag{A11}$$

Consequently, the adsorbate electron's creation operator is obtained as

$$\begin{aligned}
a^\dagger(t) &= \exp \left\{ i \int_{t_0}^t dt' [\tilde{\varepsilon}_a(t') + i\Delta(t')] \right\} a^\dagger(t_0) \langle X^\dagger(t_0)X(t) \rangle \\
&+ \int_{t_0}^t dt' \exp \left\{ i \int_{t'}^t d\tau [\tilde{\varepsilon}_a(\tau) + i\Delta(\tau)] \right\} \\
&\times \sum_k \bar{V}_{ak}^*(t') B(t - t') \exp[i\varepsilon_k(t' - t_0)] c_k^\dagger(t_0).
\end{aligned} \tag{A12}$$

Using (A11) and (A12), the occupation number of the adsorbate is obtained from the expectation values of the adsorbate electron operators

$$\langle n_a(t) \rangle = \langle a^\dagger(t)a(t) \rangle. \tag{A13}$$

In evaluating (A13), the terms proportional to $\langle a^\dagger(t_0)c_k(t_0) \rangle$ and $\langle c_k^\dagger(t_0)a(t_0) \rangle$ are equal to zero since the adsorbate and metal electrodes electrons are assumed to be decoupled at a distant past ($t_0 \rightarrow -\infty$). After some algebraic manipulations and changing the summation over k into an integration over ε , we recover (17) as,

$$\langle n_a(t) \rangle = \int d\varepsilon f(\varepsilon) \left| \int_{t_0}^t dt' \sqrt{\frac{\Delta(t')}{\pi}} B(t') \exp \left\{ -i \int_{t'}^t d\tau [E_a(\tau) - \varepsilon] \right\} \right|^2. \tag{A14}$$

where $f(\varepsilon_k) = \langle c_k^\dagger(t_0)c_k(t_0) \rangle$ is Fermi-Dirac distribution of the metal electrons, and $E_a(t) \equiv \tilde{\varepsilon}_a(t) - i\Delta(t)$. To this end, we neglected the product of the first terms of (A12) and (A11) which is a rapidly decaying transient.

Appendix B: Numerical Evaluation

In the position representation, the occupation number can be written as

$$\langle n_a(z) \rangle = \frac{1}{v^2} \int d\varepsilon f(\varepsilon) |p(\varepsilon, z)|^2. \tag{B1}$$

$p(\varepsilon, z)$ is defined as

$$p(\varepsilon, z) = \int_{z_0}^z dz' \sqrt{\frac{\Delta(z')}{\pi}} B(z') \exp \left\{ -\frac{i}{v} \int_{z'}^z dz'' [\tilde{\varepsilon}_a(z'') - i\Delta(z'') - \varepsilon] \right\}, \quad (\text{B2})$$

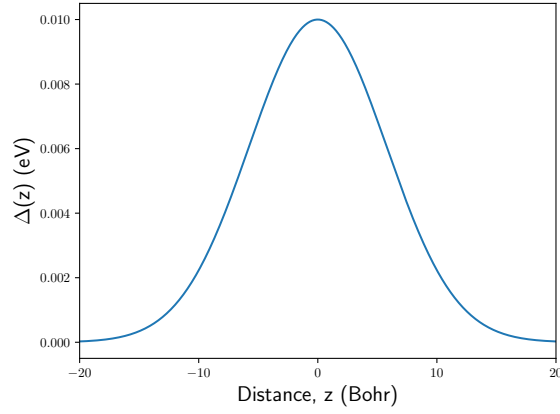
where we replaced the time dependence in the bath correlation function with z . Since $B(t)$ is maximum when $t = 0$ and approaches 1 when $t \rightarrow \infty$, we shift $B(z)$ by $z + |z_{min}|$ with $z_{min} = -20$ Bohr being the starting point in the incoming portion of the trajectory to account for this behavior. We do not consider adsorption and assume that the parameters $\Delta(z)$ and $\tilde{\varepsilon}_a(z)$ can be expressed as Gaussian functions (see (44)).

Figure 7 shows the resonance width and the energy level of adsorbate as functions of z . Our chosen parameters correspond to a system consisting of an initially empty adsorbate orbital with an energy ε_∞ that is shifted upwards by the reorganization energy due to e-ph coupling. As the adsorbate approaches near the electrode, the energy level starts to be filled when $\tilde{\varepsilon}_a(z) = \varepsilon_F$ and broadened by a magnitude Δ until $z = 0.0$ Bohr where it is at maximum. As the adsorbate moves away from the electrode, this level gradually becomes unoccupied again and returns to its value ε_∞ as $z \rightarrow \infty$.

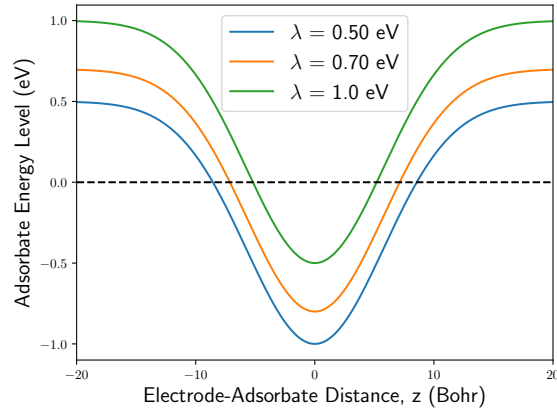
We numerically evaluate (B1) by taking the derivative of (B2) and integrating the resulting first-order complex differential equation,

$$\frac{dp(\varepsilon, z)}{dz} = \sqrt{\frac{\Delta(z)}{\pi}} B(z) - \frac{i}{v} [\tilde{\varepsilon}_a(z) - i\Delta(z) - \varepsilon] p(\varepsilon, z). \quad (\text{B3})$$

We assume that the electron transfer occurs at $T = 300$ K and integrate (B3) over the trajectory that starts at $z = -20$ Bohr and ends at $z = 20$ Bohr with the interval $\Delta z = 0.01$ Bohr using the complex ODE module of PYTHON. The initial condition corresponds to an empty adsorbate orbital at $z = -20$ Bohr. The energy integration is performed from -10 eV to 10 eV with a grid size of 0.001 eV. We consider different adsorbate velocities which includes $v = 0.23 \alpha_0 \text{eV}$, $v = 0.1 \alpha_0 \text{eV}$, $v = 0.01 \alpha_0 \text{eV}$, and $v = 0.001 \alpha_0 \text{eV}$. $v = 0.23 \alpha_0 \text{eV}$ is the thermal velocity of an adsorbate with mass $m = 1$ a kinetic energy equal to the thermal energy. In the absence of acceleration induced internally by the potential energy landscape of the adsorbate path and other external forces, this velocity may represent an upper limit in our study. The corresponding round trip simulation times $t = \frac{\hbar|z|}{v}$ for our chosen velocities are 114.5 fs, 263.3 fs, 2.633×10^3 fs, and 2.633×10^4 fs, respectively. As one may expect, the correlation function $B(t)$ requires a significant number of Matsubara frequencies $N_k \approx 10^3$ at low temperatures and can significantly slow down the calculations. However, when the



(a)



(b)

FIG. 7: (a) The adsorbate level resonance width $\Delta(z)$ for $\Delta = 0.01$ eV and $\alpha = 0.015 \alpha_0^{-2}$. (b) The adsorbate energy level $\tilde{\epsilon}_a(z)$ for different strengths of reorganization energy λ . Other parameters are $\epsilon_F = 0.0$ eV, $\kappa = \alpha$, $\epsilon_0 = -1.5$ eV and $\epsilon_\infty = \epsilon_F$. The dashed black line corresponds to the electrode's Fermi level.

electron transfer occurs at room temperature as is the case here, we found that it is sufficient to use $N_k = 2$.

Appendix C: Marcus Theory Limit

The electron transfer rate in the Marcus theory limit can be derived by first performing Fourier transform of the Lorentzian PDOS in (20) and writing the rate as

$$k = \frac{2\Delta}{\pi} \int d\varepsilon f(\varepsilon) \int_{-\infty}^{\infty} dt e^{-\Delta|t|} e^{-i(\tilde{\varepsilon}_a - \varepsilon)t}. \quad (C1)$$

Performing the thermal average as discussed in [10, 49] of (C1) with respect to bath phonons results in

$$k = \frac{2\Delta}{\pi} \int d\varepsilon f(\varepsilon) \int_{-\infty}^{\infty} dt e^{-\Delta|t|} e^{-i(\varepsilon_a + \lambda - \varepsilon)t} e^{-\frac{\lambda}{\beta} t^2}. \quad (C2)$$

Marcus theory assumes that $k_B T \gg \Delta$ which is equivalent to neglecting Δ in the exponential in (C2). Evaluating the time integral leads to the familiar Gaussian form of k as

$$k = \frac{2\Delta}{\pi} \int d\varepsilon f(\varepsilon) \sqrt{\frac{\pi}{4\lambda k_B T}} \exp \left\{ -\frac{[\varepsilon_a + \lambda - \varepsilon]^2}{4\lambda k_B T} \right\}. \quad (C3)$$

Appendix D: Derivation of Energy Exchange Rate

In order to arrive at (22), we first take the time derivative of (2) giving

$$\dot{\tilde{H}} = \dot{\tilde{\varepsilon}}_a(t) a^\dagger(t) a(t) + \sum_k \left[\dot{V}_{ak}(t) X^\dagger(t) a^\dagger(t) c_k(t) + h.c. \right]. \quad (D1)$$

To this end, the corresponding equations of motion for each operators have been used. After some algebraic manipulations, (D1) may be expressed as

$$\dot{\tilde{H}} = \dot{\tilde{\varepsilon}}_a(t) a^\dagger(t) a(t) + \frac{\dot{\Delta}(t)}{2\Delta(t)} \sum_k \left[V_{ak}(t) X^\dagger(t) a^\dagger(t) c_k(t) + h.c. \right]. \quad (D2)$$

From the equations of motion of a^\dagger and c_k ,

$$a^\dagger(t) c_k(t) = \frac{1}{V_{ak}(t) X^\dagger(t)} \left[i a^\dagger(t) \dot{a}(t) - \tilde{\varepsilon}_a(t) a^\dagger(t) a(t) \right], \quad (D3)$$

which yields

$$\dot{\tilde{H}} = \dot{\tilde{\varepsilon}}_a(t) a^\dagger(t) a(t) - \frac{\dot{\Delta}(t)}{\Delta(t)} \tilde{\varepsilon}_a(t) a^\dagger(t) a(t) + \frac{\dot{\Delta}(t)}{\Delta(t)} \Re \left[i a^\dagger(t) \dot{a}(t) \right]. \quad (D4)$$

Using (A12) and the derivative of (A11),

$$\begin{aligned} i a^\dagger(t) \dot{a}(t) &= E_a(t) a^\dagger(t) a(t) + i \sum_k c_k^\dagger(t_0) c_k(t_0) |V_{ak}|^2 \int_{t_0}^t dt' u(t) u(t') X(t) X^\dagger(t) \\ &\times \exp \left\{ i \left[\int_{t'}^t E_a^*(t'') dt'' + \varepsilon_k(t' - t) \right] \right\} + \exp \left[i \int_{t_0}^t E_a^*(t') dt' \right] a^\dagger(t_0) c_k(t_0), \end{aligned} \quad (D5)$$

Substituting (D5) into (D4) and taking the expectation value, we obtain an expression for the energy transfer rate as

$$\begin{aligned}\dot{\mathcal{E}} &\equiv \langle \dot{\hat{H}} \rangle = \dot{\tilde{\epsilon}}_a(t) \langle n_a(t) \rangle + \frac{\dot{\Delta}(t)}{\Delta(t)} \Re \left[i \int d\varepsilon f(\varepsilon) \sqrt{\frac{\Delta(t)}{\pi}} p^*(\varepsilon, t) \right], \\ &= \dot{\tilde{\epsilon}}_a(t) \langle n_a(t) \rangle + \frac{\dot{\Delta}(t)}{\sqrt{\pi\Delta(t)}} \int d\varepsilon f(\varepsilon) \Im [p(\varepsilon, t)]\end{aligned}\tag{D6}$$

with

$$p(\varepsilon, t) \equiv \int_{t_0}^t dt' \sqrt{\frac{\Delta(t')}{\pi}} B(t') \exp \left\{ i \int_{t'}^t dt'' [E_a(t'') - \varepsilon] \right\}.\tag{D7}$$

To this end, we note that the expectation value of the last term of (D5) is zero for $t_0 = -\infty$.

-
- [1] R. A. Marcus, *The Journal of Chemical Physics* **43**, 679 (1965).
 - [2] N. S. Hush, *The Journal of Chemical Physics* **28**, 962 (1958).
 - [3] V. Levich, *Physical Chemistry. An Advanced Treatise*, edited by H. Eyring, D. Henderson, and W. Jost, Vol. Xb (Academic Press, 1970).
 - [4] W. Schmickler, *J. Electroanal. Chem* **204**, 31 (1986).
 - [5] A. C. Hewson and D. M. Newns, *Japanese Journal of Applied Physics* **13**, 121 (1974).
 - [6] P. H. Citrin and D. R. Hamann, *Physical Review B* **15**, 2923 (1977).
 - [7] X. Song and R. A. Marcus, *The Journal of Chemical Physics* **99**, 7768 (1993).
 - [8] K. L. Sebastian, *The Journal of Chemical Physics* **90**, 5056 (1989).
 - [9] B. B. Smith and J. T. Hynes, *The Journal of Chemical Physics* **99**, 6517 (1993).
 - [10] J.-H. Mohr and W. Schmickler, *Physical Review Letters* **84**, 1051 (2000).
 - [11] S. Tanaka and C. P. Hsu, *Journal of Chemical Physics* **111**, 11117 (1999).
 - [12] A. M. Wodtke, J. C. Tully, and D. J. Auerbach, *International Reviews in Physical Chemistry* **23**, 513 (2004).
 - [13] E. J. Piechota and G. J. Meyer, *Journal of Chemical Education* **96**, 2450 (2019).
 - [14] R. Brako and D. M. Newns, *Surface Science* **108**, 253 (1981).
 - [15] A. Blandin, A. Nourtier, and D. Hone, *Journal de Physique* **37**, 369 (1976).
 - [16] A. Yoshimori, H. Kawai, and K. Makoshi, *Progress of Theoretical Physics Supplement* **80**, 203 (1984).
 - [17] H. Kasai and A. Okiji, *Surface Science* **183**, 147 (1987).

- [18] A. Yoshimori and K. Makoshi, *Progress in Surface Science* **21**, 251 (1986).
- [19] M. S. Mizielinski, D. M. Bird, M. Persson, and S. Holloway, *Journal of Chemical Physics* **122** (2005).
- [20] R. Brako and D. M. Newns, *Solid State Communications* **33**, 713 (1980).
- [21] M. Plihal and D. C. Langreth, *Journal of Chemical Physics* **149** (2018).
- [22] D. M. Newns, *Surface Science* **171**, 600 (1986).
- [23] H. Kasai and A. Okiji, *Surface Science* **242**, 394 (1991).
- [24] A. Gross and W. Brenig, *Chemical Physics* **177**, 497 (1993).
- [25] Y. C. Lam, A. V. Soudackov, and S. Hammes-Schiffer, *Journal of Physical Chemistry Letters* **10**, 5312 (2019).
- [26] W. Dou and J. Subotnik, *Journal of Physical Chemistry A* **124**, 757 (2020).
- [27] A. C. Hewson and D. M. Newns, *Journal of Physics C: Solid State Physics* **13**, 4477 (1980).
- [28] Z. Z. Chen, R. Lü, and B. F. Zhu, *Physical Review B - Condensed Matter and Materials Physics* **71** (2005).
- [29] A.-P. Jauho, N. S. Wingreen, and Y. Meir, *Physical Review B* **50**, 5528 (1994).
- [30] D. Langreth, *Linear and Non Linear Electron Transport in Solids*, nato asi series b ed., edited by J. T. Devreese and E. van Doren, Vol. 17 (Plenum, 1976) p. 3.
- [31] M. M. Odashima and C. H. Lewenkopf, *Physical Review B* **95** (2017).
- [32] J. X. Zhu and A. V. Balatsky, *Physical Review B* **67** (2003).
- [33] Y. Tanimura and R. Kubo, *Journal of the Physical Society of Japan* **58**, 101 (1989).
- [34] Y. Tanimura, *Physical Review A* **41**, 15 (1990).
- [35] Y. Tanimura, *Journal of Chemical Physics* **153** (2020).
- [36] N. Lambert, T. Raheja, S. Cross, P. Menczel, S. Ahmed, A. Pitchford, D. Burgarth, and F. Nori, *Physical Review Research* **5**, 013181 (2023).
- [37] D. C. Langreth and P. Nordlander, *PHYSICAL REVIEW B* **43**, 2541 (1991).
- [38] N. S. Wingreen, K. W. Jacobsen, and J. W. Wilkins, *Physical Review B* **40**, 11834 (1989).
- [39] W. Dou and J. E. Subotnik, *Journal of Chemical Physics* **148** (2018).
- [40] R. Brako and D. M. Newns, *J. Phys. C: Solid State Phys* **14**, 3065 (1981).
- [41] K. Schönhammer and O. Gunnarsson, *Physical Review B* **22**, 1629 (1980).
- [42] K. Schönhammer, *Z. Phys. B-Condensed Matter* **45**, 23 (1981).

- [43] A. M. Kuznetsov, *Physical Chemistry: An Advanced Treatise*, edited by B. E. Conway, R. J. White, and J. O. Bockris, Vol. 20 (Plenum, 1989).
- [44] W. Schmickler, *Interfacial Electrochemistry* (Oxford University, 1996).
- [45] E. Santos, M. T. Koper, and W. Schmickler, *Chemical Physics Letters* **419**, 421 (2006).
- [46] E. Santos, M. T. Koper, and W. Schmickler, *Chemical Physics* **344**, 195 (2008).
- [47] H. Nakanishi, H. Kasai, and A. Okiji, *Surface Science* **197**, 515 (1988).
- [48] A. Hamelin and M. J. Weaver, *J. Electroanal. Chem.* **223**, 171 (1987).
- [49] W. Schmickler, *Surface Science* **295**, 43 (1993).